

Received October 29, 2019, accepted November 15, 2019, date of publication November 25, 2019, date of current version December 10, 2019.

Digital Object Identifier 10.1109/ACCESS.2019.2955377

# Measurement of PM<sub>2.5</sub> Mass Concentration Using an Electrostatic Particle Concentrator-Based Quartz Crystal Microbalance

NHAN DINH NGO<sup>id</sup>, JAEGIL LEE<sup>id</sup>, MYEONG-WOO KIM<sup>id</sup>, AND JAESUNG JANG<sup>id</sup>

Sensors and Aerosols Laboratory, School of Mechanical, Aerospace and Nuclear Engineering, Ulsan National Institute of Science and Technology (UNIST), Ulsan 44919, South Korea

Corresponding author: Jaesung Jang (jjang@unist.ac.kr)

This work was supported by the 2019 Research fund (1.190011.01) of UNIST.

**ABSTRACT** Particulate matter (PM) is one of the most critical air pollutants, and various instruments have been developed to measure PM mass concentration. Of these, quartz crystal microbalance (QCM) based instruments have received much attention. However, these instruments are subject to significant drawbacks: particle bounce due to poor adhesion, need for frequent cleanings of the crystal electrode, and non-uniform distribution of collected particles. In this study, we present an electrostatic particle concentrator (EPC)-based QCM (qEPC) instrument capable of measuring the mass concentration of PM<sub>2.5</sub> (PM smaller than 2.5 μm), while avoiding the drawbacks. Experimental measurements showed high collection efficiencies (~99% at 1.2 liters/min), highly uniform particle distributions for long sampling periods (up to 120 min at 50 μg/m<sup>3</sup>), and high mass concentration sensitivity [0.068(Hz/min)/(μg/m<sup>3</sup>)]. The enhanced uniformity of particle deposition profiles and mass concentration sensitivity were made possible by the unique flow and electrical design of the qEPC instrument.

**INDEX TERMS** Quartz crystal microbalance, electrostatic particle concentrator, mass concentration, PM<sub>2.5</sub>, particulate matter sensor.

## I. INTRODUCTION

Major air pollutants include particulate matter (PM), ozone (O<sub>3</sub>), nitrogen dioxide (NO<sub>2</sub>) and sulfur dioxide (SO<sub>2</sub>) [1]. PM is a complex mixture of solid and/or liquid particles consisting of acids, organic chemicals, metals, and dust particles [2]. It is classified into coarse, fine, and ultrafine particles in terms of the aerodynamic diameter [3]. Among these, particles with an aerodynamic diameter smaller than 2.5 μm (PM<sub>2.5</sub>) are of great concerns because these particles are able to penetrate deeply into the alveoli, thereby impair lung functions [4]. Furthermore, studies in animal models have revealed that PM<sub>2.5</sub> can enter into the bloodstream, making detrimental effects on the cardiovascular system [5]. Therefore, it is critical to measure the concentration of PM<sub>2.5</sub> in the ambient atmosphere.

Based on the 24-hour average of mass concentration, there are several air quality index (AQI) levels in the primary

The associate editor coordinating the review of this manuscript and approving it for publication was Yasar Amin<sup>id</sup>.

air quality standard for PM<sub>2.5</sub> in the United States. The mass concentration in a range  $\leq 12 \mu\text{g}/\text{m}^3$  can be considered the good level,  $12.1 \mu\text{g}/\text{m}^3$ – $35.4 \mu\text{g}/\text{m}^3$  moderate level,  $35.5 \mu\text{g}/\text{m}^3$ – $55.4 \mu\text{g}/\text{m}^3$  unhealthy level for sensitive people groups,  $55.5 \mu\text{g}/\text{m}^3$ – $150.4 \mu\text{g}/\text{m}^3$  unhealthy level, and  $\geq 150.5 \mu\text{g}/\text{m}^3$  very unhealthy level [6], [7].

A wide range of instruments based on the mechanical (e.g. weighing filters, quartz crystal microbalance (QCM), tapered element oscillating microbalances), light scattering, radioactive (e.g. beta attenuation), and electrical principles (e.g. scanning mobility particle sizer) have been developed to measure the PM<sub>2.5</sub> mass concentration [8]. These instruments possess sufficient sensitivity for environment monitoring; however, they remain expensive, bulky, time-consuming, and/or labor intensive [9].

Recently, micro/nanofabrication technologies were used for aerosol sensors, particularly for low mass concentration [9]. They are capable of being integrated into daily used electronic devices, along with low production costs because of batch-operated manufacturing processes. However, they

have several drawbacks: complicated fabrication processes, poor sampling efficiency, and sensitiveness to the ambient conditions such as pressure, temperature, and relative humidity, which may lead to inaccurate measurements [9].

In order to avoid the drawbacks of bulky and miniaturized instruments, QCM-based aerosol sensors have been developed, and they are considered an appropriate candidate for the measurement of mass concentration of PM [10], [11] because the resonant frequency shift is directly proportional to the mass stuck to the oscillating (electrode) region of a QCM. In addition, the QCM possesses high sensitivity, rapid response, low cost as well as portability for on-site measurements, and have been easily integrated into aerosol instruments for both mass concentration [9], [10], [12]–[19], and mass distribution [20]–[23].

QCM-based instruments can be classified into two major categories based on particle capture mechanism: (i) inertial impaction [10], [14], [15], [19], [24], and (ii) external force based impaction (e.g. electrostatic force) [12], [13], [17], [18], [25], [26]. In the first one, the sensing electrode of the quartz crystal works as an impaction plate. Airborne particles are sampled into the sensing chamber and then deposited onto the crystal electrode by means of inertial force. However, particle bouncing and non-uniform mass distribution are the most challenges of these instruments. Even though the dislodging of particles can be reduced by coating the crystal electrode with a thin film of adhesive material (e.g., a viscous solution [12], grease [19], photoresist [15], and hydrogel [24]), this remedy still causes several problems. Those include non-linear behaviour due to overloads on a quartz crystal, an increase in measurement error because of the adsorption of other gases and vapors on the coating, and difficulty in cleaning the surfaces periodically because of adhesive coating [27].

For these reasons, the QCM was combined with the electrostatic precipitator (ESP) [12], [13], [17], [18]. These instruments possess advantages in comparison with the inertial impaction-based QCMs. They showed high collection efficiencies, low particle losses on the chamber walls [18], and the high adhesive force between the particles and the surface, causing the particles to stick firmly to the surface [18], [27]. However, non-uniform mass distribution is a classic weakness not only in the traditional instruments but also in the QCM-ESP instruments. Indeed, airborne particles begin depositing relatively uniformly onto the electrode surface; however, as deposition continues, incoming airborne particles tend to deposit near the center of the QCM electrode. Therefore, mass loading increases much faster at the center of the crystal's electrode than at the outer edge [12], leading to non-uniform and multiple layers of deposited particles, and hence non-linearity in the frequency shift with an increase in mass deposited on the crystal. Therefore, quartz crystals have to be cleaned frequently [17], and the sampling process needs to be conducted in a short period. Last but not the least, all previous QCM-ESP instruments were designed based on a “point-to-plane” configuration, and if the point-to-plane

distance is short, electrical sparking may occur frequently, resulting in damage to the quartz crystal [17].

In this study, we developed a novel instrument for PM<sub>2.5</sub> measurements by integrating QCM with an electrostatic particle concentrator (EPC) for particle sampling [28], which is referred to as the qEPC instrument. In the qEPC, two outlets were placed next to the inlet, and its side, bottom, and top walls were biased to the electrical ground except for the center of the bottom wall, where a quartz crystal was located, enhancing the electric field strength over the quartz crystal, which worked as the collection spot and was connected to the negative DC voltage, and concentrating aerosols evenly on the quartz crystal. Owing to its unique design, the qEPC instrument was able to provide (i) high collection efficiencies and (ii) uniform particle distribution for a long period of time or high particle concentrations, resulting in a longer sampling period before cleaning. This can overcome the shortcomings of the present QCM-ESP instruments.

## II. SIMULATION AND EXPERIMENTS

The collection efficiency of the qEPC was simulated with COMSOL Multiphysics 5.4 software (COMSOL Inc.). The experimental set-up for qEPC evaluation consisted of the aerosol generation system, the qEPC, and a commercial measurement instrument. Methods for counting particles collected on the crystal electrode as well as for quartz crystal calibration, and performance tests were also described.

### A. INSTRUMENT DESIGN, SIMULATION, AND FABRICATION

The qEPC instrument was designed to concentrate target particles evenly on the electrode of a QCM crystal for mass concentration measurements. It was designed to be of portable size, simple operation, and to have low power consumption. The general design of the qEPC instrument was similar to the personal EPC described by our previous study [28]. More specifically, a 5MHz QCM crystal (QCM5140CrAu120-050-Q, Quartz Pro AB, Sweden) was fixed by a crystal holder which was placed on the bottom part of the qEPC. The top electrode (diameter = 12mm) of the QCM crystal served as both a collection plate and a measuring electrode. An inlet (diameter = 8.9mm) and two outlets (diameter = 4.8mm) were placed on the top. Both the top and bottom part were made of aluminum, while the crystal holder was made of acrylic.

A three dimensional (3D) simulation model of the qEPC instrument was built and computed in COMSOL Multiphysics 5.4 software. This task aimed to confirm the physical sampling efficiencies, particle motion inside the instrument, and particle distribution on the crystal electrode. Geometry module and its add-on were used to create a 3D simulation domain. Electrostatic and laminar flow modules were used to model the electrical field and airflow, respectively. Particle tracing for fluid flow module was used for computing the particle motion under the electric and flow fields with electrical, drag, gravity, and Brownian forces imbedded.

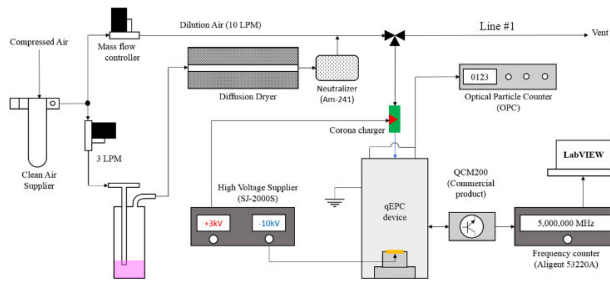


**FIGURE 1.** Experimental setup for evaluating the performances of the qEPC device.

The qEPC instrument was then designed in the SolidWorks 2015 software, and fabricated at the Machine shop at UNIST. In addition, a BME280 sensor (Bosch Sensortec GmbH) was integrated into the qEPC instrument for temperature, humidity, and pressure measurements to account for the environmental effects on the frequency measurements.

**B. AEROSOL AND QCM SYSTEM**

The experimental setup for evaluation of the qEPC instrument is shown in Fig. 1. Air was supplied using a clean air supplier (Dekati, Finland). The airflow was divided into two lines. One was fed to a three-jet Collison nebulizer (Mesa Laboratories, Denver, CO) for generating airborne monodisperse polystyrene particles from a liquid suspension at a flow rate of 3 liters per minute (LPM). These red fluorescent polymer microspheres (Thermo Scientific, US) were 0.5μm, 0.8μm and 2.0μm in diameter. The uniformity and measured mean diameter of 0.8μm particles were less than 3% and 0.79 μm, and those of 2.0μm particles were less than 5% and 2.1μm, respectively. The particles generated from the nebulizer were dried in a diffusion dryer (HCT, South Korea), neutralized in a diffusion neutralizer (5.622, GRIMM, Germany) equipped with a radioactive source (Am-241) to make the Boltzmann charge distribution, and then diluted with clean air coming from the other line of clean air source. All airflow rates were controlled by mass flow controllers (5850E, Brooks Instrument, PA). The mass concentration of the generated aerosols was varied from 29.57 μg/m<sup>3</sup> to 190.63 μg/m<sup>3</sup>, and from 39.27 μg/m<sup>3</sup> to 183.01 μg/m<sup>3</sup> for 2.0 μm, and 0.8 μm, respectively.

Aerosolized particles were extracted from the mainline (Line #1) to the qEPC at a fixed flow rate of 1.2 LPM, and the extracted particles were corona-charged at a voltage of +3kV (SJ-2000S, Sejin electronics, Korea). The positively charged particles were introduced through the inlet and were collected to the quartz crystal electrode via electrostatic force generated by the qEPC. There are two operation modes: capture mode and measurement mode. In the capture mode, the top crystal electrode served as a collection plate, which was wired to -10kV (SJ-2000S, Sejin electronics Korea) for high electrical field generation. In the measurement mode, this electrode acted as a QCM crystal electrode. Thus, it was connected to an oscillation circuit for frequency shift measurement. The shift

in frequency was measured by a frequency counter (53220A, KeySight Technologies, US), and a quartz crystal controller (QCM200, Stanford Research Systems, US). The LabVIEW 2014 (National Instrument) was used for frequency acquisition from the frequency counter. The number and mass concentration of airborne particles were also measured with an optical particle counter (OPC) (1.109, GRIMM, Germany).

Frequency measurements started with connecting the qEPC to the QCM controller. Frequency signals were recorded for initial 10 min as reference signals without sampling. The qEPC was then disconnected from the QCM controller. Aerosolized particles were introduced through the corona charger for 5 min. The charged particles were fed to the qEPC, and the high voltage supplier (-10kV) was turned on for capturing charged particles onto the quartz crystal electrode. Finally, the high voltage source was removed, and the qEPC was re-connected with the QCM controller followed by recording frequency values, the measurement signals. The frequency shifts were calculated by subtracting the measurement signals from the reference signals.

**C. METHODS FOR qEPC EVALUATION**

In addition to the OPC, the mass concentration of airborne particles can be obtained from counting the number of particles collected on the QCM crystal electrode. An optical microscope (Nikon Eclipse 80i) equipped with a mono color camera (CoolSNAP™ DYN0 CCD Camera, PHOTOMETRIC®) was used to image the deposited particles on the crystal electrode. The number of particles on these captured images was counted by ImageJ software (Wayne Rasband, version 1.52e, USA). The total deposited mass, *m*, was then calculated by the following formula:

$$m = N_p V_p \rho_p \tag{1}$$

where *N<sub>p</sub>* is the number of particles deposited on the quartz crystal electrode, which was determined by the fluorescence microscopy, *V<sub>p</sub>* is the volume of a single particle, *ρ<sub>p</sub>* is particle density (*ρ<sub>p</sub>* = 1060 kg/m<sup>3</sup>). Since the total mass is known, the mass concentration (*C*) was determined by

$$C \left[ \frac{\mu g}{m^3} \right] = \frac{m [\mu g]}{Q \left[ \frac{m^3}{min} \right] t [min]} \tag{2}$$

where *Q* is the volumetric flow rate, and *t* is sampling time.

The collection efficiency is a primary consideration of air samplers, and two methods for measuring this property were described. The first method is to evaluate the collection efficiency for various particle sizes (0.5μm, 0.8μm, and 2.0μm for PM<sub>2.5</sub>) at a fixed mass concentration (60μg/m<sup>3</sup>) of aerosolized samples. The collection efficiency was calculated based on the particle number concentration measured at the outlets of the qEPC:

$$\eta_1 [\%] = \frac{N_{E=0V} - N_{E=-10kV}}{N_{E=0V}} \tag{3}$$

where *N<sub>E=0V</sub>* and *N<sub>E=-10kV</sub>* are the number concentrations measured at the outlet without electric field and with

applying  $-10\text{kV}$ , respectively. Moreover, the qEPC instrument was designed to measure the mass concentration of PM<sub>2.5</sub>, and the collection efficiencies were measured with various mass concentrations, ranging from  $30\mu\text{g}/\text{m}^3$  to  $260\mu\text{g}/\text{m}^3$  for each particle size,  $0.8\mu\text{m}$  and  $2.0\mu\text{m}$ . The collection efficiency was estimated based on the mass concentrations measured at the outlets of the qEPC devices:

$$\eta_2 [\%] = \frac{C_{E=0V} - C_{E=-10kV}}{C_{E=0V}} \quad (4)$$

where  $C_{E=0V}$  and  $C_{E=-10kV}$  are the mass concentrations measured at the outlet without electric field and with applying  $-10\text{kV}$ , respectively.

For the measurement of mass sensitivity and particle distribution with different mass over the crystal electrode, aerosolized particles with a fixed mass concentration ( $\sim 50\mu\text{g}/\text{m}^3$ ) were tested at different periods ranging from 5 min to 120 min. The deposited mass attached on the crystal was calculated by using (1).

### III. RESULTS AND DISCUSSIONS

In this section, we present the collection efficiency [%], mass sensitivity [ $\text{Hz}/\mu\text{g}$ ], mass concentration sensitivity [ $(\text{Hz}/\text{min})/(\mu\text{g}/\text{m}^3)$ ], and particle distribution profiles of the qEPC. The collection efficiency is a primary consideration of any particle samplers. Mass sensitivity was obtained by experiments and compared with prediction by the Sauerbrey equation [18]. Moreover, the mass concentration sensitivity was measured with two sizes of PM<sub>2.5</sub>. Lastly, particle distribution profiles with sampling time over the entire quartz crystal electrode were presented.

#### A. FREQUENCY MEASUREMENTS OF THE qEPC INSTRUMENT

It is well known that the Sauerbrey equation gives a linear relationship between the shift in the resonant frequency of a quartz crystal and the mass deposited on it. However, this relationship is valid only when the deposited thin and rigid film is uniformly and tightly distributed on the crystal [10], [18], [29]. Thus, the rigidity of attached particles on a quartz crystal surface can be estimated via frequency responses of the crystal [30], [31].

Figure 2 shows the frequency shifts measured during ten-minute measurement modes before and after particle capture at various mass concentrations of aerosolized samples. The frequency shifts during the measurements were nearly constant at all tested mass concentrations, where their standard deviations were 0.5 Hz at both particle sizes, because particles were rarely captured, reflecting the high level of adhesive forces between the captured particles and the crystal electrode. This observation is important for further tests of the qEPC instrument because of the following reasons. In the capture mode, the charged particles were carried to the crystal surface by a combination of inertial and electrical forces, causing the particles to stick firmly to the crystal electrode [18]. However, in the measurement mode, the quartz

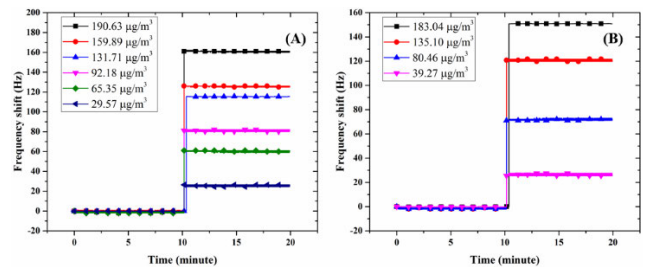


FIGURE 2. The measured frequency shifts of the QCM crystal with respect to time for two particle sizes: (A)  $2.0\mu\text{m}$ , and (B)  $0.8\mu\text{m}$ , where the frequencies of the measurement modes before and after particle capture were merged.

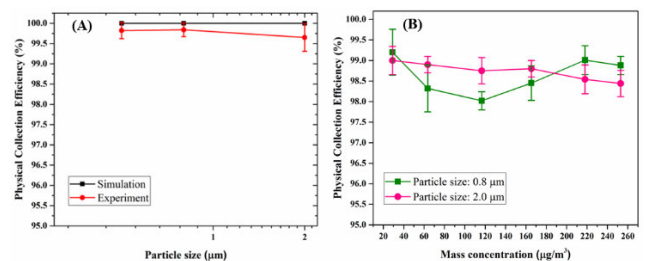


FIGURE 3. (A) The collection efficiencies of the qEPC for different particle sizes of PM<sub>2.5</sub> ( $0.5\mu\text{m}$ ,  $8\mu\text{m}$ , and  $2.0\mu\text{m}$ ). (B) The experimental collection efficiencies of the qEPC for various mass concentrations of aerosolized samples ( $0.8\mu\text{m}$  and  $2.0\mu\text{m}$ ;  $30\mu\text{g}/\text{m}^3$ – $260\mu\text{g}/\text{m}^3$ ). The experimental collection efficiencies were calculated based on the particle number concentration measured at the outlet of the qEPC via (3).

crystal was disconnected from the high voltage supply. Thus, an absence of electrical field might cause the weak interaction between adhered particles and crystal surface and result in the positive frequency shift of a quartz crystal, leading to the measurement inaccuracy [31].

#### B. COLLECTION EFFICIENCY

As the sensitivity of the qEPC depends on particle capture on the quartz crystal electrode, it is essential to achieve the collection efficiency of the qEPC as highly as possible for a variety of particle sizes and mass concentration of aerosolized samples. Figure 3 shows the collection efficiencies of the qEPC obtained by simulation and experiments. The collection efficiencies of both the numerical simulations and experimental measurements were very close and they were more than 99.6% for all the tested particle sizes (Fig. 3A). In several studies having similar geometric designs to the qEPC [28], [32], the collection efficiencies were almost 100% for  $0.1\mu\text{m}$ – $10\mu\text{m}$  diameter [28] and 99.3–99.8% for  $0.05\mu\text{m}$ – $2\mu\text{m}$  diameter particles [32]. It should be noted here that the qEPC possessed differences in its design compared to those similar ones, because the quartz crystal electrode was used in the qEPC as a collection plate and was 12 mm in diameter. This is much smaller than the collection plate sizes in Dixkens and Fissan (25 mm in diameter) [32], and Hong et al. (20 mm in diameter) [28], both of which did not involve quartz crystal electrodes.



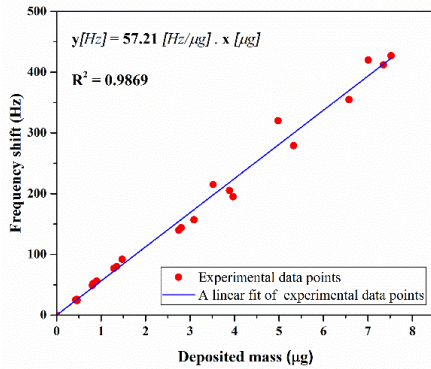


**FIGURE 4.** Experimental mass sensitivity of the quartz crystal used in the qEPC where the deposited mass was calculated by (1). The mass sensitivity based on the Sauerbrey equation was 50Hz/µg for the 5MHz QCM crystal used in this study.

The particle collection efficiency of an ESP can also be affected by the concentration of the aerosols to be collected. In fact, the high concentration of aerosolized particles can cause a decrease in the ion volume charge concentration [33], reducing the overall particle collection. Therefore, the physical collection efficiency of the qEPC for a wide range of mass concentrations was also investigated (Fig. 3B). The collection efficiency was shown to be nearly 99% under various mass concentration ranges, from 30 µg/m<sup>3</sup> to 260 µg/m<sup>3</sup>, which is a very high concentration for PM<sub>2.5</sub>.

It should be noted that these physical collection efficiencies were based on the particle concentrations measured at the outlets of the qEPC, which is a convenient and commonly used way to measure the collection efficiency. However, this collection efficiency did not reflect the number of particles captured on other areas than the QCM crystal electrode. In fact, some particles were deposited on the qEPC wall and QCM crystal holder. For the qEPC, we found that the losses were 11.2% of the particles coming into the EPC.

**C. MASS SENSITIVITY**

Mass sensitivity of a quartz crystal plays a crucial role in the practical application of QCM. Figure 4 shows the frequency shift (Hz) as a function of loaded mass (µg) for 2µm particle size. The experimental mass sensitivity (57Hz/µg) was very close to, but slightly larger than, that predicted by the Sauerbrey equation (50Hz/µg), indicating that the deviation was 7 (Hz/µg), corresponding to 14%. This difference is larger than the value (10%) reported in SEM et al. [10]. However, the Sauerbrey equation does not consider the properties of adhered particles such as particle size, particle to surface bonding, their chemical properties, etc. Moreover, there is no simple and exact relationship between the accumulated mass and the frequency shift of a quartz crystal, and the frequency response depends on the particle collection device, particle size, and the physical and chemical properties of the aerosol particles [27]. In fact, many previous studies showed a quite amount of discrepancies between experimental and

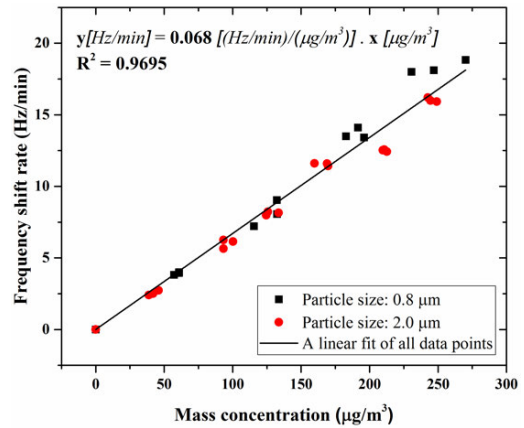


**FIGURE 5.** Experimental mass concentration sensitivity of the qEPC instrument based on the OPC measurements.

the Sauerbrey equation predicted mass sensitivities for different aerosol samples. An office aerosol test, for example, showed that the theoretical and experimental values were 177(Hz/µg) and 198(Hz/µg), respectively, resulting in a difference of 11% [18]. The tests of ambient laboratory pollution also showed a difference of 32% [16].

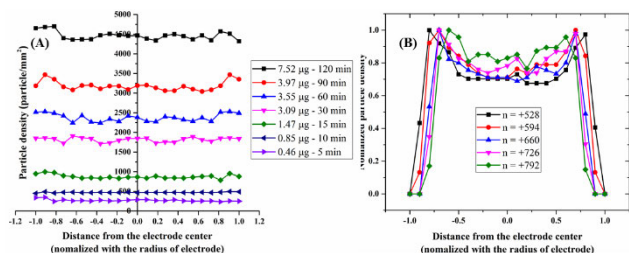
**D. MASS CONCENTRATION SENSITIVITY**

Figure 5 shows the relationship between the mass concentration measured by the OPC and the resonant frequency shift of the quartz crystal. The linear fit with the zero intercept for all qEPC measurements of these two particle sizes indicates that the mass concentration sensitivity was 0.068 (Hz/min)/(µg/m<sup>3</sup>) and R-square value (R<sup>2</sup>) was 0.9695. This mass concentration sensitivity was greater than that obtained from an impaction-based QCM [0.0554 (Hz/min)/(µg/m<sup>3</sup>)] [33], which is due to the fact that the qEPC had higher particle collection efficiencies because of high electrostatic attraction. In addition, the data obtained by the OPC were close to those obtained from fluorescence measurements on the quartz crystal, where the mass concentration sensitivity was 0.070 (Hz/min)/(µg/m<sup>3</sup>) and R-square value (R<sup>2</sup>) was 0.9729.

**E. PARTICLE DEPOSITION DISTRIBUTION**

One of the critical requirements for the QCM-based instruments is that loaded mass needs to be uniformly deposited on the crystal electrode to get high linearity for a wide range of mass [18]. However, it is not possible to achieve complete uniformity of captured mass in real applications, especially in PM measurement, as reported in previous studies [12], [18], [34]. Thus, it is recommended that higher uniformity of particle deposition should be made over the entire crystal electrode for linearity at longer sampling time or larger deposited mass [35].

Figure 6 shows the profiles of particle density measured on the quartz crystal electrode. The y-axes show the particle density or normalized particle density based on the experiments



**FIGURE 6.** (A) Experimental particle density profiles on the crystal electrode for different total mass deposited on it at  $50\mu\text{g}/\text{m}^3$ . (B) Particle density profiles based on COMSOL simulation for a variety of elementary charge levels ( $n$ ). The particle densities were measured for areas of  $0.295\text{ mm}^2$  for (A) and  $0.785\text{ mm}^2$  for (B).

(fluorescence microscopy) and simulations, and the x-axes show the measured spots, which were normalized with the electrode radius. From the experimental data (Fig. 6A), it is clear that the profiles were almost uniform over the crystal electrode with various loaded mass (or sampling time); however, the particle densities near the edges were slightly higher than those at the center of the electrode. The profiles were also simulated by COMSOL (Fig. 6B), and the simulated profiles showed similar patterns to those measured in the experiments for a variety of elementary charge levels of the particles. The number of simulated elementary charges of  $2\mu\text{m}$  diameter particles was varied from +528 to +792, and their experimentally observed average value was +693.

The uniformity of particle deposition profiles was made possible by the fluidic and electrical design of the qEPC instrument. Briefly, when pre-charged particles are guided into the qEPC chamber through the inlet, the flow expands in the streamwise direction, reducing its velocity. These particles were transported to a section above the QCM crystal surface, where the flow velocity was low enough for the particles to be electrically captured on the crystal because the boundary layer thickness of the flow was large far downstream from the inlet [28], [32]. Moreover, the bottom wall was biased to the ground to increase the electric field intensity over the quartz crystal [28]. In fact, flow velocity at the center of the aerosol jet coming out of the inlet was higher than that at its edge, and the difference of these two velocities decreased with the streamwise direction [32]. A low flow rate (e.g. 0.3 LPM) gave more uniform particle deposition than a high flow rate (e.g. 2.4 LPM) [32]; however, as the velocity of particles decreased, the deposition zone shrank toward the center of electrode because of higher electrical mobility of particles [32]. This may cause a local deposition, which can be controlled by adjusting the flow rate, electric field intensity, and corona charging.

Another problem in particle sampling is that multiple layers might occur on the collection electrode, decreasing mass sensitivity owing to the weak interaction between the layers [36]. Thus, we looked into the microscopic deposition of particles by scanning electron microscopy (SEM) images on the crystal electrode (Fig. 7). Due to the chosen geometry of the qEPC, the deposition of particles charged with the corona

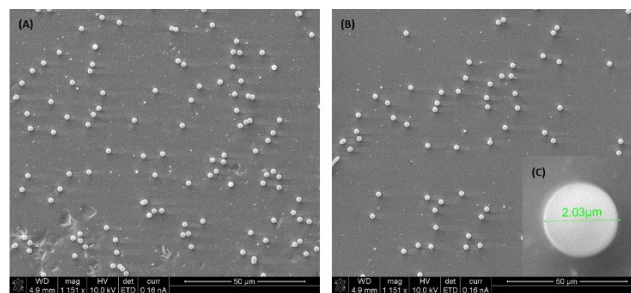


**FIGURE 7.** (A) A scanning electron microscope-imaged particles of  $2\mu\text{m}$  in diameter deposited on a crystal electrode (B) at the center with (C) a single deposited particle. The scale bar is  $50\mu\text{m}$ .

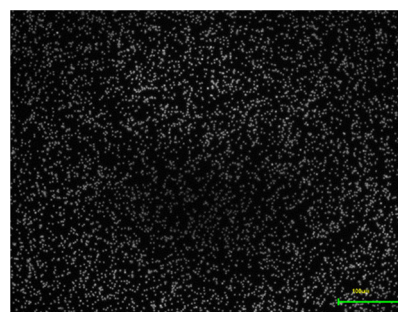


**FIGURE 8.** An optical microscope image of  $2\mu\text{m}$  diameter particles deposited on a QCM crystal electrode. (At the center zone of the crystal electrode; using lens 20X). The scale bar is  $100\mu\text{m}$ .

charger will be approximately independent of the particle diameter [32]. Here, the particle size of  $2\mu\text{m}$  was chosen as the PM<sub>2.5</sub> representative for this observation. From the SEM images, it is clear that most of the particles in the layer were deposited as a monolayer on the QCM crystal electrode at both the boundaries (Fig. 7A) and the center area (Fig. 7B) when the particles were sampled for 120 min, corresponding to  $7.52\mu\text{g}$ . In addition, the macroscopic distribution of loaded particles on the QCM crystal electrode was imaged with a fluorescence microscope (Fig. 8), where most of the particles was uniformly and singly distributed.

#### IV. CONCLUSION

In this study, we have presented the design and fabrication of an EPC-based QCM (qEPC) instrument for the measurement of PM<sub>2.5</sub> mass concentration, and experimentally characterized its performances with a highly accurate commercial OPC. The qEPC enhanced the electric field strength over the quartz crystal working as the collection spot and concentrated aerosols evenly on the quartz crystal. The experimental characterizations showed the advantages of the qEPC instrument: high collection efficiencies ( $\sim 99\%$  at 1.2 LPM), high linearity ( $R^2 = 0.9695$ ) in a mass concentration range  $< 260\mu\text{g}/\text{m}^3$ , more uniform particle distributions and hence longer sampling time before cleaning (up to 120 min at  $50\mu\text{g}/\text{m}^3$ ), and high mass concentration sensitivity [ $0.068(\text{Hz}/\text{min})/(\mu\text{g}/\text{m}^3)$ ]. We are now developing an instrument to measure the mass concentration of a variety of

aerosol matters (e.g. PM, and bioaerosol particles) in real-time based on this topology.

## REFERENCES

- [1] WHO Air Quality Guidelines for Particulate Matter, Ozone, Nitrogen Dioxide and Sulfur Dioxide, World Health Org., Geneva, Switzerland, 2006.
- [2] EPA, Washington, DC, USA. (2018). *Particulate Matter (PM) Basics*. Accessed: Dec. 24, 2018. [Online]. Available: <https://www.epa.gov/pm-pollution/particulate-matter-pm-basics#PM>
- [3] M. Sierra-Vargas and L. M. Teran, "Air pollution: Impact and prevention," *Respirology*, vol. 17, no. 7, pp. 1031–1038, Oct. 2012.
- [4] Y.-F. Xing, Y.-H. Xu, M.-H. Shi, and Y.-X. Lian, "The impact of PM<sub>2.5</sub> on the human respiratory system," *J. Thoracic Disease*, vol. 8, no. 1, pp. E69–E74, Jan. 2016.
- [5] A. Nemmar, H. Vanbilloen, M. F. Hoylaerts, P. H. M. Hoet, A. Verbruggen, and B. Nemery, "Passage of intratracheally instilled ultrafine particles from the lung into the systemic circulation in hamster," *Amer. J. Respiratory Crit. Care Med.*, vol. 164, no. 9, pp. 1665–1668, Nov. 2001.
- [6] *Air Quality Index—A Guide to Air Quality and Your Health*, document EPA-456/F-14-002, 2014.
- [7] *The National Ambient Air Quality Standards for Particle Pollution Revised Air Quality Standards for Particle Pollution and Updates to the Air Quality Index (AQI)*, United States Environ. Protection Agency (EPA), Washington, DC, USA, 2012.
- [8] S. S. Amaral, J. A. De Carvalho, Jr., M. A. M. Costa, and C. Pinheiro, "An overview of particulate matter measurement instruments," *Atmosphere*, vol. 6, no. 9, pp. 1327–1345, Sep. 2015.
- [9] U. Soysal, E. Géhin, E. Algré, B. Berthelot, G. Da, and E. Robine, "Aerosol mass concentration measurements: Recent advancements of real-time nano/micro systems," *J. Aerosol Sci.*, vol. 114, pp. 42–54, Dec. 2017.
- [10] J. G. Olin and G. J. Sem, "Piezoelectric microbalance for monitoring the mass concentration of suspended particles," *Atmos. Environ.*, vol. 5, no. 8, pp. 653–668, Aug. 1971.
- [11] K. Kaur, R. Mohammadpour, I. C. Jaramillo, H. Ghandehari, C. Reilly, R. Paine, and K. E. Kelly, "Application of a quartz crystal microbalance to measure the mass concentration of combustion particle suspensions," *J. Aerosol Sci.*, vol. 137, Nov. 2019, Art. no. 105445.
- [12] G. J. Sem, K. Tsurubayashi, and K. Homma, "Performance of the piezoelectric microbalance respirable aerosol sensor," *Amer. Ind. Hygiene Assoc. J.*, vol. 38, no. 11, pp. 580–588, Nov. 1977.
- [13] G. J. Sem and K. Tsurubayashi, "A new mass sensor for respirable dust measurement," *Amer. Ind. Hygiene Assoc. J.*, vol. 36, no. 11, pp. 791–800, Jun. 1975.
- [14] R. L. Chuan, "An instrument for the direct measurement of particulate mass," *J. Aerosol Sci.*, vol. 1, no. 2, pp. 111–113, Jan. 1970.
- [15] J. Zhao, M. Liu, L. Liang, W. Wang, and J. Xie, "Airborne particulate matter classification and concentration detection based on 3D printed virtual impactor and quartz crystal microbalance sensor," *Sens. Actuators A, Phys.*, vol. 238, pp. 379–388, Feb. 2016.
- [16] *Kanomax 3521 Piezobalance Aerosol Mass Monitor (10, 4 μm)*. Accessed: Dec. 27, 2018. [Online]. Available: <https://www.jjstech.com/3521.html>
- [17] L. W. Wilson, M. J. Hefner, D. Reilly, and J. D. C. Jones, "Development of a personal dust monitor with a piezoelectric quartz crystal sensor," *Meas. Sci. Technol.*, vol. 8, no. 2, pp. 128–137, Feb. 1997.
- [18] J. G. Olin, G. J. Sem, and D. L. Christenson, "Piezoelectric-electrostatic aerosol mass concentration monitor," *Amer. Ind. Hygiene Assoc. J.*, vol. 32, no. 4, pp. 209–220, Apr. 1971.
- [19] E. Zampetti, A. Macagnano, P. Papa, A. Bearzotti, F. Petracchini, L. Paciucci, and N. Pirrone, "Exploitation of an integrated microheater on QCM sensor in particulate matter measurements," *Sens. Actuators A, Phys.*, vol. 264, pp. 205–211, Sep. 2017.
- [20] M. Chen, F. J. Romay, L. Li, A. Naqwi, and V. A. Marple, "A novel quartz crystal cascade impactor for real-time aerosol mass distribution measurement," *Aerosol Sci. Technol.*, vol. 50, no. 9, pp. 971–983, Jul. 2016.
- [21] D. Wallace and R. Chuan, "Cascade impaction instrument using quartz crystal microbalance sensing elements for real-time particle size distribution studies," IBC, Irvine, CA, USA, Tech. Rep. CONF-760985-Journal ID: CODEN: XNBSA, 1977. [Online]. Available: <https://www.osti.gov/biblio/6385530-cascade-impaction-instrument-using-quartz-crystal-microbalance-sensing-elements-real-time-particle-size-distribution-studies>
- [22] *Quartz Crystal Microbalance QCM MOUDI Impactor Model 140*, TSI Incorporated, Shoreview, MN, USA, 2019.
- [23] W. Stöber, F. J. Mönig, H. Flachsbarth, and N. Schwarzer, "Mass distribution measurements with an aerosol centrifuge with quartz sensors as mass detectors," *J. Aerosol Sci.*, vol. 10, no. 2, p. 232, Jan. 1979.
- [24] D. Liang, W.-P. Shih, C.-S. Chen, and C.-A. Dai, "A miniature system for separating aerosol particles and measuring mass concentrations," *Sensors*, vol. 10, no. 4, pp. 3641–3654, Apr. 2010.
- [25] *Piezobalance Respirable Aerosol Mass Monitor 8510*. Accessed: Dec. 27, 2018. [Online]. Available: <https://www.tsi.com/discontinued-products/piezobalance-respirable-aerosol-mass-monitor-8510/>
- [26] *Piezobalance Dust Monitor 3521-22 Series at Kanomax USA*. Accessed: Dec. 27, 2018. [Online]. Available: <https://www.kanomax-usa.com/product/piezobalance-dust-monitor-3520-series/>
- [27] C. Lu and A. W. Czanderna, *Applications of Piezoelectric Quartz Crystal Microbalances*. Amsterdam, The Netherlands: Elsevier, 1984.
- [28] S. Hong, J. Bhardwaj, C.-H. Han, and J. Jang, "Gentle sampling of sub-micrometer airborne virus particles using a personal electrostatic particle concentrator," *Environ. Sci. Technol.*, vol. 50, no. 22, pp. 12365–12372, Nov. 2016.
- [29] F. Tan, X. Huang, S. Zhou, and C. Qing, "Phase and mass relationship of the QCM sensor coated with rigid thin film," in *Proc. Int. Conf. Commun., Circuits Syst. (ICCCAS)*, Nov. 2013, pp. 376–380.
- [30] C. Gu, P. Li, F. Jin, G. Chen, and L. Ma, "Effects of the imperfect interface and viscoelastic loading on vibration characteristics of a quartz crystal microbalance," *Acta Mech.*, vol. 229, no. 7, pp. 2967–2977, Jul. 2018.
- [31] P. Castro, P. Resa, and L. Elvira, "Apparent negative mass in QCM sensors due to punctual rigid loading," *IOP Conf. Ser., Mater. Sci. Eng.*, vol. 42, no. 1, Dec. 2012, Art. no. 012046.
- [32] J. Dixkens and H. Fissan, "Development of an electrostatic precipitator for off-line particle analysis," *Aerosol Sci. Technol.*, vol. 30, no. 5, pp. 438–453, Nov. 1999.
- [33] Y. Wang, Y. Wang, D. Chen, X. Liu, C. Wu, and J. Xie, "A miniature system for separation and detection of PM based on 3-D printed virtual impactor and QCM sensor," *IEEE Sensors J.*, vol. 18, no. 15, pp. 6130–6137, Aug. 2018.
- [34] V. A. Marple, B. Y. H. Liu, and G. A. Kuhlmeier, "A uniform deposit impactor," *J. Aerosol Sci.*, vol. 12, no. 4, pp. 333–337, Jan. 1981.
- [35] J. R. Vig and A. Ballato, "Comments on the effects of nonuniform mass loading on a quartz crystal microbalance," *IEEE Trans. Ultrason., Ferroelectr., Freq. Control*, vol. 45, no. 5, pp. 1123–1124, Sep. 1998.
- [36] M. H. Ho, "Applications of quartz crystal microbalances in aerosol mass measurement," *Methods Phenomena*, vol. 7, pp. 351–388, Jan. 1984.



**NHAN DINH NGO** received the B.Eng. degree in mechanical engineering from the Da Nang University of Technology, Da Nang, Vietnam, in 2013. He is currently pursuing the Ph.D. degree with the Sensors and Aerosols Laboratory, School of Mechanical, Aerospace and Nuclear Engineering, Ulsan National Institute of Science and Technology (UNIST), Ulsan, South Korea. His research interests include microelectromechanical systems (MEMS) design and process, and quartz crystal microbalance (QCM)-based sensors for aerosol/bioaerosol applications.



**JAEGIL LEE** received the B.S. degree in mechanical design engineering from the Kumoh National Institute of Technology, South Korea, in 2019. He then joined the Sensors and Aerosols Laboratory, Ulsan National Institute of Science and Technology (UNIST). His research interest includes aerosol sampling systems.



**MYEONG-WOO KIM** received the B.S. degree in mechanical engineering from the Ulsan National Institute of Science and Technology (UNIST), Ulsan, South Korea, in 2016. He then joined the Sensors and Aerosols Laboratory, UNIST. His research interest includes bioaerosol sampling systems.



**JAESUNG JANG** received the B.S. and M.S. degrees in mechanical engineering from the Pohang University of Science and Technology (POSTECH), Pohang, South Korea, in 1997 and 1999, respectively, and the Ph.D. degree in mechanical engineering from Purdue University, West Lafayette, IN, USA, in 2004. From 2004 to 2007, he worked as a Postdoctoral Research Associate for the development of cantilever biosensors for the detection of airborne viruses at the School of Electrical and Computer Engineering, Purdue University, West Lafayette, IN, USA. After serving as an Assistant Professor with Chung-Ang University, Seoul, South Korea, he joined the faculty of the Department of Mechanical Engineering, Ulsan National Institute of Science and Technology (UNIST), Ulsan, South Korea, in 2010, where he is currently an Associate Professor. His research interests include capture, manipulation, concentration, separation, and measurement of airborne particles, especially for airborne biological particles.

• • •